Appl. Chem. Eng., Vol. 21, No. 3, June 2010, 265-271

축전식 이온제거에 대한 TiO_2/Activated Carbon 화합물의 전기흡착 거동

이정원 · 김홍일 · 김한주 · 박수길†

충북대학교 공업화학과
(2009년 11월 10일 접수, 2010년 2월 25일 채택)

Electrosorption Behavior of TiO_2/Activated Carbon Composite for Capacitive Deionization

Jeong-Won Lee, Hong-Il Kim, Han-Joo Kim, and Soo-Gil Park†

Department of Industrial Engineering Chemistry, Chungbuk National University, Cheongju 361-763, Korea
(Received November 10, 2009; Accepted February 25, 2010)

활성탄에 TiO_2를 졸-겔 방법으로 코팅하여 탄소복합전극을 제조하였고 축전식 이온제거(Capacitive deionization : CDI) 과정에서 나타난 제염효과에 대하여 고찰하였다. 본 연구에서 TiO_2는 전극의 젖음성을 향상시켜 전극과 전해질의 접촉저항을 감소시키고, 전기이중층 흡착량을 증가시킬 수 있으므로 CDI전극재로 활성탄에 코팅하였다. TEM, XRD, XPS로 활성탄에 TiO_2가 코팅되었는지 확인하였다. 순환전류전압법과 impedance측정 결과 탄소복합전극이 탄소전극보다 전기이중층 용량이 증가하였으며, 전극의 확산저항이 줄어든 것을 확인하였다. 또한 이온제거율을 확인하기 위한 충전-방전 및 이온전도도 평가 결과 전해질 NaCl 1000 μS/cm에서 탄소복합전극이 탄소전극보다 39% 더 많은 이온을 제거하는 것을 확인하였다. 본 연구 결과 CDI용 전극재료 TiO_2가 코팅된 탄소복합전극이 탄소전극보다 효과적인 제염효과를 보임을 확인하였다.

Desalination effects of capacitive deionization (CDI) process was studied using TiO_2/activated carbon electrode. In order to enhance the wettability of electrode and decrease a electrode resistance, TiO_2 was coated on activated carbon. By means of TiO_2 coating on activated carbon, electric double layer to adsorption content in CDI process was increased. It was identified from TEM, XRD, and XPS that the activated carbon based on TiO_2 composite was fabricated successfully by means of sol-gel method. As a results of cyclic voltammetry and impedance, it was identified that TiO_2/activated carbon electrode has more electric double later capacitance and less diffusion resistance than activated carbon. Also charge-discharge and ion conductivity profiles showed that the ion removal ratios of TiO_2/activated carbon electrode in NaCl electrolyte of 1000 μS/cm more increased about 39% than that of activated carbon. In conclusion it was possible to identify that the carbon electrode coated TiO_2 as electrode material was more effective than raw carbon electrode.

Keywords: *capacitive deionization, desalination, activated carbon, TiO_2*

1. Introduction

Water, as a precious natural resource, plays an important part in people's life on the planet. The demand for clean and fresh water is ever increasing for many reasons including population growth, industrial development and severe draught in some parts of the globe. The continuing and the change of rainfall patterns in Korea compel the innovative research to examine new sources of water to supplement traditional supplies. The total content of water existing the earth is about 1.38 billion km^3. The 97.5% of 1.38 billion km^3 is salty water which can be easy acquired. So, it is necessary for desalination which can solve water shortages. Desalination has been developed to turn salt water into fresh water. The main conventional processes used include by following : reverse osmosis, thermal evaporation and electrodialysis processes[1-3]. These methods have some advantages and disadvantages. In reverse osmosis membrane system, a high-pressure pump is used and it is very difficult to maintain the constant permeate flux of the membrane, remove fouling and scaling. The evaporation method has been used for a long time because the operating principle and equipment are very simple and high purity fresh water can be obtained. However, its disadvantage is that the energy cost is very high. The electrodialysis method uses an ion-exchange membrane and needs high voltage to treat the water in salt solution of high concentration. Therefore, it is usually used for the treatment of low concentration brine. A promising answer to overcome the high energy cost problem is electrosorption[4-7].

† 교신저자 (e-mail: sgpark@cbnu.ac.kr)

Capacitive deionization (CDI) process operates by sequestering ions in the electric double layer near charged surfaces. Essentially, a solution included ions flows through a highly porous conducting pair of electrodes. Anions or other negatively charged species are removed at the positive electrode while cations or positively charged species are separated from solution at the negative electrode[8]. Charged ions are held in the double layer, and once the electric field is removed, the ions are quickly released back to the bulk solution. Because of this reversibility, capacitive deionization offers several advantages over other conventional technologies. Unlike ion exchange, in capacitive deionization salt solution are only required for regeneration of the surface, thereby substantially reducing the amount of secondary waste. Compared with thermal processes, such as evaporation the electrosorption consumes less energy to achieve similar results. CDI also has operational advantages over electrodialysis and reverse osmosis because no membranes are required[9-12].

Practical CDI systems date back to fundamental work on porous carbon electrodes by Johnson and Newman in 1971[8]. Unfortunately, this concept for desalinating water lay fallow until the mid 1990's. While working on high surface area conducting carbon aerogels, Farmer et al[4,8,13] at Lawrence Livermore National Labs (LLNL) developed the first capacitive desalination device. Most current CDI systems employ high surface area conducting carbon in a variety of forms. These forms can be carbon aerogels[4,8,10,12], carbon cloths[14], sheets of carbon[15], or more contemporary carbon nanotubes and nanofibers[16].

When a constant electric potential is applied to activated carbon electrodes for a period of time, the adsorbed amount of NaCl is defined as physical adsorption, and the adsorbed amount of NaCl under an electric field－as electric adsorption[17]. For a given quantity of activated carbon, a large electric field adsorption leads to a more effective electrosorption performance. Therefore, the surface modification is required to enhance its electric field adsorption so as to reduce its physical adsorption. Since polar groups of activated carbon work as adsorption sites for physical adsorption, and introduction of metal atoms through the reaction between metal alkoxide molecules and polar groups reduces physical adsorption[18]. Moreover, an enhancement of electric field adsorption can be expected if the polarity of introduced metal atoms is altered with applying electric potential.

In this study, To increase electric potential the TiO_2 of anatase structure was coated on activated carbon using sol-gel method. TiO_2 exists in different polymorphic forms, such as rutile and anatase. The crystal structures of TiO_2. The rutile and anatase were express TiO_2 octahedron chain that Ti^{4+} was surrounded by six O^{2-} in common. The crystal structures were distinguish by a difference on warp of octahedron and repeated structure. The O^{2-} ion octahedron of rutile was represent in minutely warped orthorhombic but anatase decreased a property of symmetric due to most warped orthorhombic than rutile. The anatase structure of TiO_2 has used on electrochemical capacitors, because it has characteristics of uniform pore, wide specific surface area and good wetting[19,20]. So, enhance wettability of electrode and decrease electrode resistance and increase electric double layer adsorption content in CDI process the anatase structure of TiO_2 was coated on activated carbon. Also, the oxidizing cathode of TiO_2 increase positive charge and the reducing anode of TiO_2 increase negative charge when the anatase of TiO_2 used as CDI electrode material. Because the ions of different polarity strongly was adsorbed around TiO_2 which can be reversibly oxidized and reduced with low potential difference the adsorption content of electric double layer was increased[21]. And we investigated for performance with TiO_2/activated carbon prepared as CDI electrode.

2. Experimental

2.1. Preparation of TiO_2/activated Carbon Composite and Electrode

The TiO_2/activated carbon material is obtained by sol-gel process. Titanium tera-isopropoxide (JUNSEI) used as a precursor of titania and 2-propanol (J.T.Baker) were commercially available with purities of 99% and 99.5%, respectively. Then they were mixed with ultrasonication for 1h to enhance dispersibility of mixed solution. In order to separate from the solvent, the mixture was drying at 120 ℃ into vacuum. The dried product was calcinated at 450 ℃ for 5 h in air to prepare TiO_2/activated carbon composite. The electrode was prepared to a rubber type of TiO_2/activated carbon composite as active material and polytetrafluoroethylene (PTFE, Aldrich) binder mixed with the weight ratio 90 : 10. The electrode pressed on graphite foil as current collector. And then it was dried under was dried under vacuum at 120 ℃ for 24 h before electrochemical measurement.

2.2. Capacitive Deionization Unit Cell Fabrication

To test CDI performance, unit cell was fabricated with the TiO_2/ activated carbon electrode. The seperator, polyethylene mesh prevent from a short and retain constant distance (0.03 mm) between identical electrodes of 8 × 8 cm^2 area. The water flow hole (diameter, 6 mm) was made in electrode. The electrodes was fixed with the acryl support and then were fabricated to two CDI unit cell.

2.3. Characterization

The Transmission Electron Microscopy (TEM, Libra 120) was used to monitor particle sized and crystallity. The crystal structure of TiO_2/ activated carbon composites were characterized by X-Ray Diffraction (XRD, D8 Discover with GADDS) and X-ray Photoelectron Spectroscopy (XPS, ESCALAB 210). The specific surface area of TiO_2/activated carbon composites were characterized by nitrogen adsorption isotherm (ASAP 2010) at 77 K. The electrochemical performance of the prepared carbon electrode is performed by Cyclic voltammetry and impedance. When it was charged or discharged in CDI unit cell the ion removal ratio analyzed with the measured ion conductivity. And then, the NaCl solution used as the electrolyte solution that the initial ion conductivity is 1000 μS/cm. The quantitative analysis was performed by Ion Chromatography which can analyze concentration of Na^+ ion.

3. Results and Discussion

Changes on morphology of TiO_2/activated carbon composite by sol-gel method were evaluated by TEM measurements. Figure 1(a)

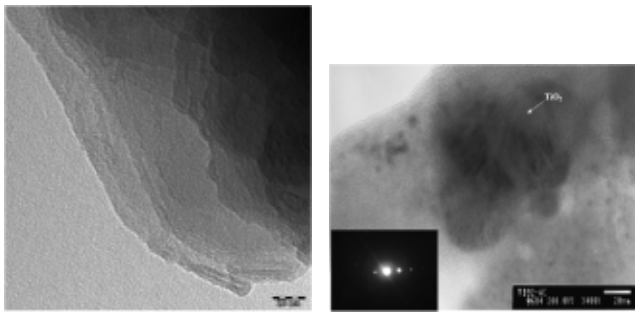

(a) (b)

Figure 1. TEM image of (a) activated carbon and (b) TEM image and electron diffraction pattern of TiO_2/activated carbon.

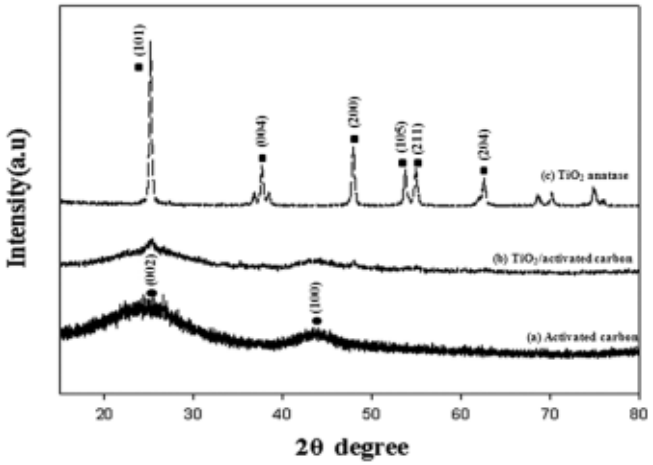

Figure 2. XRD patterns of (a) activated carbon (b) TiO_2/activated carbon (JCPDS file no. 21-1272) composite and (c) TiO_2 anatase.

present TEM image of activated carbon. Figure 1(b) present TEM image and electron diffraction pattern of TiO_2/activated carbon. In TEM image of Figure 1(b) it was identified that the TiO_2 coated with size of 60∼80 nm in activated carbon. The X-ray diffraction image showed that TiO_2 had crystallity[22].

The crystal structure of activated carbon and TiO_2/activated carbon composite were characterized by XRD. Figure 2 shows the XRD patterns for activated carbon and TiO_2/activated carbon. In XRD pattern result of activated carbon depicted in Figure 2(a) that we identified (002) peak and (100) peak existed conventional carbon[23]. In XRD pattern, the result of TiO_2/activated carbon depicted in Figure 2(b) that it was showed (101), (004), (200), (105), (211) and (204) peaks existed the TiO_2 anatase structure of activated carbon (JCPDS file no. 21-1272)[24]. Consequently, it was identified that structure of TiO_2/activated carbon composite prepared with sol-gel method is the anatase of TiO_2.

The XPS analysis have been performed to investigate the chemical bonding state of Ti in the TiO_2/activated carbon composite shown in Figure 3. The high resolution of C1s spectrum in Figure 3(b) has been resolved into three individual component peaks representing C-C bind (B.E. = 284.6 eV) as the major peak, O-C=O bind (B.E. = 288.11 eV) and C-O bind (B.E. = 286.5 eV). The curve-fitting results of C1s spectrum are approximately in agreement with the previous data[25,26]. As shown in Figure 3(c), binding energies of $Ti2_{p1/2}$ and $Ti2_{p3/2}$ are 464.5 and 458.8 eV, respectively, which can been assigned to the Ti^{4+} (TiO_2) with a peak separation of 5.7 eV between those two peaks[27,28]. The obtained O1s spectrum shown in Figure 3(d) has following three chemical states of oxygen corresponding to Ti–O bind of TiO_2 (B.E. = 529.7 eV), C–O bind (B.E. = 533.3 eV) and OH^- bind (B.E. = 531.6 eV), which can be compared to the published data[28-30]. The hydroxyl groups on the surface of TiO_2 can be attributed to reaction of adsorbed H_2O with TiO_2 and formation of Ti–OH, such as H_2O + Ti–O–Ti → 2Ti–OH[31].

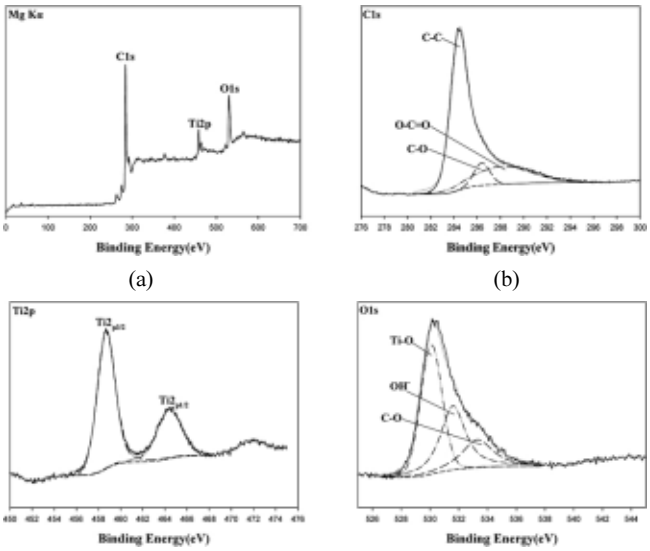

Figure 3. XPS spectrum of (a) TiO_2/activated carbon and XPS core spectra of each elements; (b) C1s, (c) Ti2p and (d) O1s.

Table 1. XPS Results of TiO_2/Activated Carbon Composite

Photocatalyst	C1s	Ti_2p	O1s
FWHM (eV)	2.10	1.90	2.60
At. (%)	60.01	7.47	32.52

FWHM : full width at a half of the maximum height of peaks.
At. : Atomic percent.

The full width at half maximum (FWHM) and atomic percent (At.) values are summarized in Table 1. The atomic% of TiO_2 particle (Cx) was calculated peak area from the Equation (1):

$$C_X atomic\% = [(I_i/F_i)/\Sigma I/F)] \times 100 \quad (1)$$

Where I is the number of photoelectron per second in a specific spectra peak, F is the atomic sensitivity factor, i is the TiO_2 element[32].

According to the XPS result, in TiO_2/activated carbon composite, TiO_2 particle was contained correctly 7.47% respectively, in Figure 3(c) and Table 1.

Figures 4, 5 present N_2 adsorption isotherm and pore distribution in

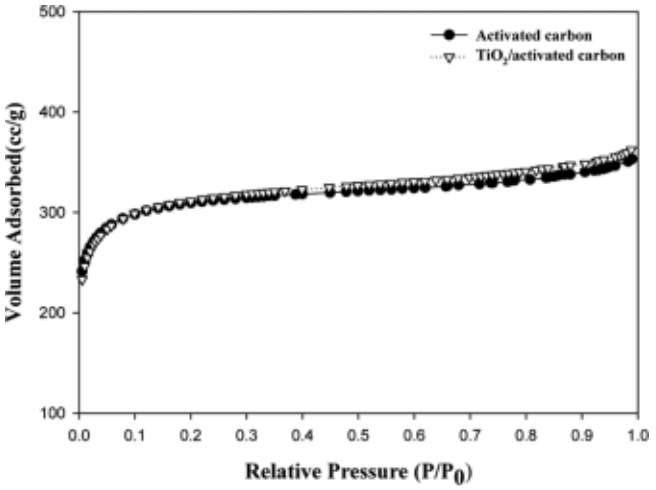

Figure 4. Comparison of nitrogen adsorption isotherms plotted on the relative pressure scale for the activated carbon and TiO_2/activated carbon composite.

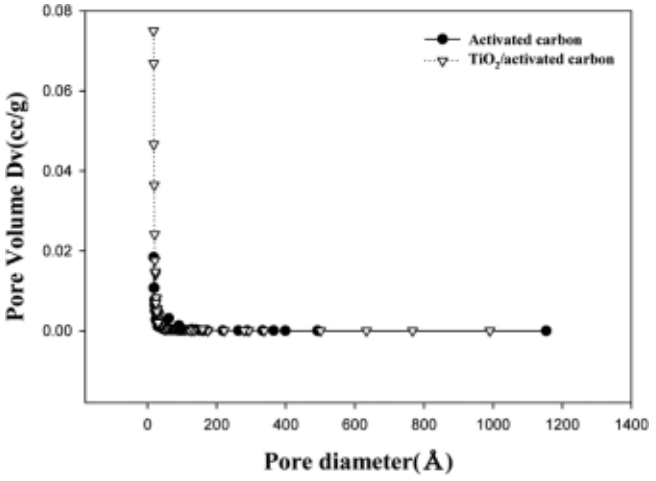

Figure 5. Pore size distributions of activated carbon and TiO_2/activated carbon using nitrogen adsorption at 77 K.

N_2 gas for activated carbon and TiO_2/activated carbon. The activated carbon and TiO_2/activated carbon using this study show Types I classified by Brunauer (Figure 4). Type I adsorption isotherms property is called to Langmuir type that the adsorption content is increased with increasing gas pressure but the adsorption content is constant regardless of gas pressure above constant pressure. That is, it was mostly showed much adsorption content in low relative pressure and above relative pressure adsorption content is not increased with increasing relative pressure since it reach absorption equilibrium which show almost horizontal behavior. As a result of nitrogen adsorption isotherms, it was identified that much micropores were existed because much adsorption content was showed in low relative pressure. Also, we identified that TiO_2/activated carbon had mesopores for ion removal because micropore region was decreased and mesopore region was increased when TiO_2 was coated on activated carbon.

In Figure 5 it was identified that micro- and meso- pores were made in activated carbon and TiO_2/activated carbon since most pore volume of activated carbon and TiO_2/activated carbon exist under 30 Å.

Table 2. Specific Surface Area and Volume of Activated Carbon and TiO_2/Activated Carbon Composite

Sample	S_{BET} (m^2/g)	S_{mi} (m^2/g)	V_{tot} (cm^3/g)	V_{mi} (cm^3/g)	D (Å)
Activated carbon	1,202.00	1,045.00	0.55	0.41	18.00
TiO_2/activated carbon	1,187.00	997.00	0.56	0.40	18.90

S_{BET} : BET surface area, S_{mi} : micropore area, V_{tot} : total volume, V_{mi} : micropore volume, D : average pore diameter

Table 3. Capacitance of Activated Carbon and TiO_2/Activated Carbon Electrode in 4 M NaCl at Various Scan Rate

Sample	1 mV/s	5 mV/s	10 mV/s
Activated carbon	125.00 F/g	106.70 F/g	92.45 F/g
TiO_2/activated carbon	151.00 F/g	125.37 F/g	108.54 F/g

Table 2 present specific surface area, average pore size and pore diameter of activated carbon and TiO_2/activated carbon. The specific surface area, average pore size of activated carbon is 1,202 m^2/g, 18 Å, respectively. The specific surface area, average pore size of TiO_2/ activated carbon is 1,178 m^2/g, 18.9 Å, respectively. The IUPAC classifies pores into three classed: micropores (diameters less than 20 Å), mesopores (diameters between 20 and 500 Å) and macropores (diameters greater than 500 Å). The macropore had only the secondary importance in practical adsorption process because macropore was provided as pathway to adsorb solute in liquid[33,34]. The ion size dissolved in water usually is 6～7.6 Å. So it is possible for adsorption in micropore of 15 Å[35]. In this study, we identified that pores of activated carbon and TiO_2/activated carbon were developed to effective pore because the micropore size of activated carbon and TiO_2/activated carbon is 18 to 8.9 Å.

The electrosorption mechanism and the electrosorptive capacitance for carbon electrode were performed by cyclic voltammetry (CV). The working electrodes had surface area of 1 × 1 cm^2. The counter and reference electrodes were of a platinum wire and Ag/AgCl/sat. KCl electrode, respectively. The electrolyte solutions used 4 M NaCl aqueous solution. The CV measurement was carried out in the potential range of -0.8～0.8 V where didn't exist oxidation and reduction reaction. Figure 6 present the results that (a) activated carbon and (b) TiO_2/ activated carbon measured at scan rates of 1, 5 and 10 mV/s. As a result of CV, activated carbon and TiO_2/activated carbon showed conventional electric double layer behavior and smooth adsorption & desorption of ions in electrode surface of those. Also, a result of comparison with each scan rates showed that the specific capacitance of TiO_2/activated carbon electrode was more increased than that of activated carbon.

Table 3 present specific capacitance by results of CV. The specific capacitance (F/g) of electrode was calculated on the basis of equation (2) that specific capacitance divide average current [(i_c+i_a)] by sweep rate (υ) and total weight of the active material in one electrode (ω) (Equation (2))[36].

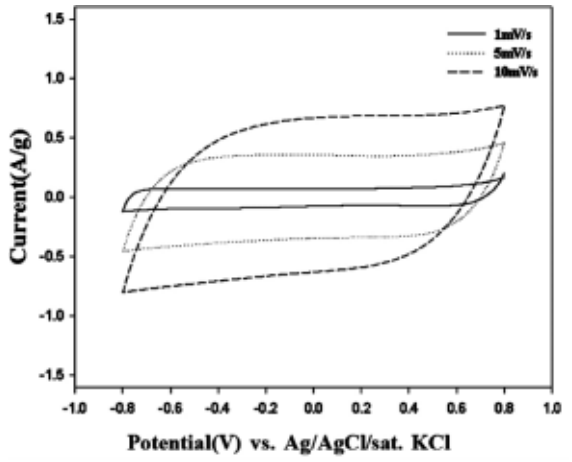

(a)

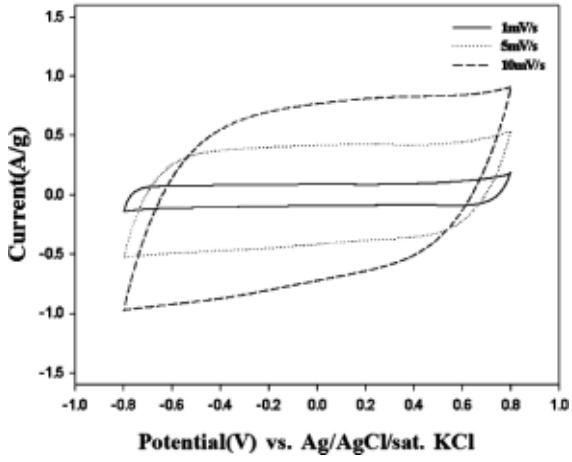

(b)

Figure 6. Cyclic voltammograms of (a) activated carbon electrode (b) TiO_2/activated carbon electrode at scan rate 1, 5 and 10 mV/s in 4 M NaCl electrolyte (vs.Ag/AgCl/sat.KCl).

$$c_s = [(i_c + i_a)/2/v]/w \quad (2)$$

It was showed in Table 3 that the specific capacitance was increased with decreasing scan rate in activated carbon and TiO_2/activated carbon electrode. It was explained that the adsorption and desorption rate is different according to the pore size existed activated carbon. That is, when the scan rate is high the low specific capacitance showed that the ions was only adsorbed to activated carbon surface since it didn't move to micropore. But when the scan rate is low the specific capacitance of activated carbon electrode increased since the ions was adsorbed to micropore of activated carbon by diffusion[37]. Therefore it is thought that the ion removal ratio may decrease with increasing flow velocity. Also, in all scan rates the TiO_2/activated carbon electrode had more specific capacitance than activated carbon electrode. As this results, when TiO_2 of prepared carbon composite electrode give potential the oxidizing TiO_2 of cathode increase positive charge and the reducing TiO_2 of anode increase negative charge. Like this, because the ions of different polarity was strongly adsorbed around TiO_2 which can be reversibly oxidized and reduced with low potential[21]. Also, When the activated carbon was coated with TiO_2 the wettability of electrode is enhanced and the diffusion resistance is decreased[38]. Consequently, it was thought that the carbon composite electrode in CDI process can be effectively remove ions.

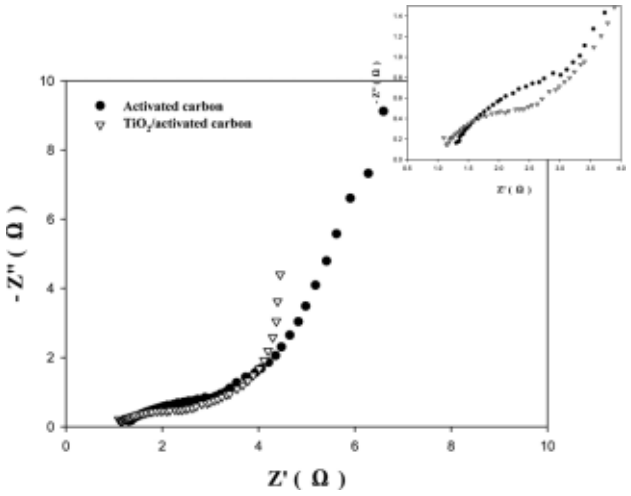

Figure 7. Nyquist plots of the activated carbon and TiO_2/activated carbon electrodes in 4 M NaCl electrolyte, Frequency range from 1 kHz to 10 mHz, Amplitude of AC potential : 10 mV.

Figure 7 shows the impedance plots of the activated carbon and TiO_2/activated carbon electrodes in 4 M NaCl electrolyte. The Nyquist polts of the activated carbon and the TiO_2/activated carbon electrodes are characteristic of semicircles in the high frequency ranges and a sloping straight line in the low frequency range. According to the previous report[39], the high frequency semicircle relates to the charge transfer through the electrode/electrolyte interface and the sloping line at low frequency reflects the solid-state diffusion of electrolyte ion in the bulk materials.

It was obviously saw from Figure 7 that the size of semicircle on TiO_2/activated carbon electrode are much smaller than that of the activated carbon electrode. The resistances of the electrode/electrolyte interface on TiO_2/activated carbon electrodes were lower than activated carbon electrode. The considerable effect of the Warburg impedance in the TiO_2/activated carbon electrode shows a good CDI-like behavior. The Warburg impedance represents that the sloping line has a special quality of the more sloping line neared at 90 ℃ where the more bulk resistance decrease. As above results, it was showed that the internal resistance of electrode was decreased because the wettability of electrode were enhanced when activated carbon coated TiO_2. The adsorption and desorption of ions were experimented in constant potential using Potentiostat (Wonatech) during flux of electrolyte. The electric conductivity of treated water was measured in ion conductivity meter (Istek Inc., 455C) installed on exit of cell.

To investigate effects for flow velocity in CDI process experiment, the electrode cells were measured for flux of 15 ml/min in NaCl (1000 μS/cm) electrolyte. The experiments were measured in unit cell where charge-discharge conditions are charge of 1.3 V, 5 min and discharge of -0.001 V, 5 min and rest time of 1min. After 5th cycle, the voltage

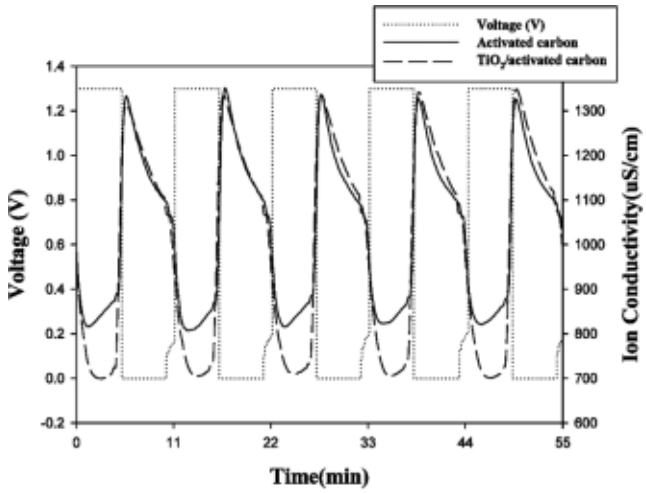

Figure 8. Adsorption/desorption profiles of activated carbon electrode and TiO_2/activated carbon electrode in NaCl 1000 μS/cm solution at 15 mL/min flow rate.

Table 4. Feed Conductivity (C_f), Lowest Product Conductivity (C_p) and Salt Removal Rate of Activated Carbon Electrode and TiO_2/ Activated Carbon Electrode in NaCl 1000 μS/cm Electrolyte

Sample	C_f	C_p	Salt removal rate (%)
Activated carbon	1,000 μS/cm	816 μS/cm	18.4%
TiO_2/activated carbon	1,000 μS/cm	700 μS/cm	30%

C_f : Feed conductivity, C_p : lowest product conductivity

vs ion conductivity graph for charge-discharge time was presented in Figure 8.

Figure 8 present voltage vs ion conductivity graph for charge-discharge time in activated carbon electrode and TiO_2/activated carbon electrode, respectively. When the electrodes were charged to potential of 1.3 V, the ion conductivity was decreased since cations and anions in electrolyte adsorb to each electrodes. But when the electrodes were discharged to potential of -0.001 V, the ion conductivity was increased since cations and anions in electrodes desorb in electrolyte. It was observed that after 5 min in starting desorption reaction the ion conductivity of electrodes reach to initial value. It was showed stable adsorption and desorption behavior of ions during 5 cycle. The ion conductivity of activated carbon electrode and TiO_2/activated carbon was 184 μS/cm, 300 μS/cm in 1 cycle, respectively. Also, the ions content removed of NaCl electrolyte in Figure 8 was calculated to percentage by equation (3)[40].

$$\text{Removal rate (\%)} = \frac{C_f - C_p}{C_f} \times 100 \quad (3)$$

In equation (3), C_f is initial ion conductivity value and C_p is lowest ion conductivity value when electrodes charge. Table 4 present content of NaCl ions removed for flow velocity.

As results of Figure 8 and Table 4, the ion removal ratios of TiO_2/activated carbon electrode in NaCl electrolyte of 1000 μS/cm more increased about 39% than that of activated carbon. Also, Table 5 present Ion Chromatography analysis with used electrolytes to quantitative analysis.

Table 5. Amount of Removed Na Cation by Activated Carbon Electrode and TiO_2/Activated Carbon Electrode

	Na^+
Amount of ion for feel electrolyte	135.72 ppm
Amount of ion removal for activated carbon electrode	25.28 ppm
Amount of ion removal for TiO_2/activated carbon electrode	38.44 ppm

In analysis results of Na^+ concentration, it was identified that the cations removal ratios of TiO_2/activated carbon electrode more increased about 52% than that of activated carbon.

When CDI electrode material was used with TiO_2 the cathode of TiO_2 was oxidated with increasing positive charge and the anode of TiO_2 was reduced with increasing negative charge. Like this, it was strongly pulled opposite charge around TiO_2 which could be reversibly oxidized and reduced with low voltage. Therefore the electric double layer adsorption content was increased. Another reason why electric double layer adsorption content was increased is decrease of internal resistance since wettability at electrode/electrolyte interface was enhanced[21]. As a result, because TiO_2 was increased electric double layer adsorption as main mechanism and decreased internal resistance in CDI process, it was identified that TiO_2/activated carbon compared with activated carbon electrode in CDI electrode can effectively be remove ions.

4. Conclusions

The activated carbon coated with TiO_2 composite was successfully fabricated by means of sol-gel method, and it was charactered by TEM, XRD, and XPS. As a result of BET it was identified that the meso porous region which could adsorb more ion content than activated carbon was increased in TiO_2/activated carbon. It was identified by cyclic voltammetry and impedance that TiO_2/activated carbon electrode has more electric double layer capacitance and less diffusion resistance than activated carbon. Comparing with activated carbon and TiO_2/activated carbon, the ion removal ratios of TiO_2/activated carbon electrode in NaCl electrolyte of 1000 μS/cm more increased about 39% than that of activated carbon. In a result of Ion Chromatography, it was identified that the Na^+ removal ratios of TiO_2/activated carbon electrode more increased about 52% than that of activated carbon. The TiO_2/activated carbon have more ion removal content than the activated carbon because the TiO_2 coated on activated carbon enhance electric double layer capacitance and wettability of electrode and reduce electrode resistance. The activated carbon coated TiO_2 as additive is effective for the considerable enhancement of its CDI process in ion removal amount.

Acknowledgements

This work was supported by the research grant of the Chungbuk National University in 2008.

References

1. J. A. Trainham and J. Newman, *J. Electrochem. Soc.*, **124**, 1528 (1977).
2. W. J. Blaedel and J. C. Wang, *Anal. Chem.*, **51**, 799 (1979).
3. M. Matlosz and J. Newman, *J. Electrochem. Soc.*, **133**, 1850 (1986).
4. J. C. Farmer, D. V. Fix, G. V. Mark, R. W. Pekala, and J. F. Poco, *J. Electrochem. Soc.*, **143**, 159 (1996).
5. A. Porteous, Desalination Technology, Applied Science Publishers, London (1983).
6. K. S. Spiegler and Y. M. El-Sayed, *Desalination*, **134**, 109 (2001).
7. R. V. Perez, M. L. Rodriguez, and J. Mengual, *Desalination*, **137**, 199 (2001).
8. J. C. Famer, D. V. Fix, G. V. Mark, R. W. Pekala, and J. F. Poco, *J. Appl. Electrochem.*, **26**, 1007 (1996).
9. T. Hori, M. Hashino, A. Omori, T. Matsuda, K. Takasa, and K. Watanabe, *J. Membr, Sci.*, **132**, 203 (1997).
10. C. M. Yang, W. H. Choi, B. W. Cho, W. I. Cho, K. S. Yun, and H. S. Han, *J. Korea Ind. Eng. Chem.*, **15**, 294 (2004).
11. J. Wang, L. Angnes, H. Tobias, R. A. Roesner, K. C. Hong, R. S. Glass, F. M. Kong, and R. W. Pekala, *Anal. Chem.*, **65**, 2300 (1993).
12. R. W. Pekala, J. C. Farmer, C. T. Alviso, T. D. Tran, S. T. Mayer, J. M. Miller, and B. Dunn, *J. Non-Cryst. Solids*, **255**, 74 (1998).
13. J. C. Farmer, S. M. Bahowick, J. E. Harrar, D. V. Fix, R. E. Martinelli, A. K. Vu, and K. L. Carroll, *Energy & Fuels*, **11**, 337 (1997).
14. T. J. Welgemoed and C. F. Schutte, *Desalination*, **183**, 327 (2005).
15. K. K. Park, J. B. Lee, P. Y. Park, S. W. Yoon, J. S. Moon, H. M. Eum, and C. W. Lee, *Desalination*, **206**, 86 (2007).
16. X. Z. Wang, M. G. Li, Y. W. Chen, R. M. Cheng, S. M. Huang, L. K. Pan, and Z. Sun, *Appl. Phys. Lett.*, **89**, 1 (2006).
17. A. Afkhami and B. E. Conway, *J. of Colloid and Interface Science*, **251**, 248 (2002).
18. L. Zou, G. Morris, and D. Qi, *Desalination*, **225**, 329 (2008).
19. B. R. Weinberger and R. B. Garber, *Appli. Phys. Lett.*, **66**, 2409 (1995).
20. Augustynski, *J. Electrochem. Acta*, **38**, 43 (1993).
21. M. W. Ryoo and G. Seo, Water Res., **37**, 1527 (2003).
22. H. Wang, Y. Wu, and B. Q. Xu, *Applied catalysis B : Environmental*, **59**, 139 (2005).
23. Y. J. Hwang, S. K. Jeong, J. S. Shin, K. S. Nahm, and A. M. Stephan, *Journal of Alloys and Compounds*, **448**, 141 (2008).
24. X. H. Xia, Z. J. Jia, Y. Yu, Y. Liang, Z. Wang, and L. L. Ma, *Carbon*, **45**, 717 (2007).
25. T. Takahagi and A. Ishitani, *Carbon*, **22**, 43 (1984).
26. M. C. Paiva, C. A. Bernardo, and M. Nardin, *Carbon*, **38**, 1323 (2000).
27. C. Wagner and G. Muilenbergy (Eds.), Handbook of X-ray Photoelectron Spectroscopy, Perkin-Elmer Corporation, Minnesota (1979).
28. F. M. Liu and T. M. Wang, *Appl. Surf. Sci.*, **195**, 284 (2002).
29. S. Biniak, G. Szymanski, J. Siedlewski, and A. Swiatkowski, *Carbon*, **35**, 1799 (1997).
30. J. G. Yu, X. J. Zhao, and Q. N. Zhou, *Thin Solid Films*, **379**, 7 (2000).
31. M. R. Hoffmann, S. T. Martin, W. Choi, and D. W. Bahnemann, *Chem. Rev.*, **95**, 69 (1995).
32. Y. M. Kim, *J. of the Korean Society of Analyrical Sciences*, (1992).
33. M. Mullier and B. Kastening, *J. Electroanal. Chem.*, **374**, 149 (1994).
34. H. Shi, *Electrochimica Acta*, **39**, 2083 (1994).
35. I. Tanahashi, A. Yoshida, and A. Nishino, *J. Electrochem. Soc.*, **137**, 3052 (1990).
36. A. J. Bard and L. R. Faulkner, Electrochemical Methods, John Wiley & Sons Inc., **522**, New York (1980).
37. C. H. Hou, C. Liang, S. Yiacoumi, S. Dai, and C. Tsouris, *J. of Colloid and Interface Science*, **302**, 54 (2006).
38. Q. Shen, S. K. You, S. G. Park, H. Jiang, D. Guo, B. Chen, and X. Wang, *Electroanalysis*, **20**, 2526 (2008).
39. J. Xie, X. B. Zhao, G. S. Cao, and M. J. Zhao, *Electrochem. Acta*, **50**, 2725 (2004).
40. J. B. Lee, K. K. Park, H. M. Eum, and C. W. Lee, *Desalination*, **196**, 125 (2006).